Effect of Al concentration on the holographic grating efficiency and ionic conductivity in sodium magnesium aluminosilicate glasses

Abdulatif Y. Hamad,* James P. Wicksted, Michael R. Hogsed,† Joel J. Martin, Charles A. Hunt, and George S. Dixon
Department of Physics and Center for Laser & Photonics Research, Oklahoma State University, Stillwater, Oklahoma 74078-3072
(Received 11 June 2001; published 22 January 2002)

A systematic study of grating formation, erasure, and decay in $15Na_2O \cdot 12MgO \cdot xAl_2O_3 \cdot (73-x)SiO_2$ glasses doped with 1.26 mol% Eu_2O_3 is reported as a function of Al_2O_3 concentration for $x=0$ to 15. The permanent change in the index of refraction was a linearly increasing function of Al_2O_3 concentration. The grating buildup and erasure rates also increased with Al_2O_3 concentrations. This is attributed to the reduced activation energy for forced diffusion of small modifiers bound to AlO_4^- clusters rather than to nonbridging oxygens. Ionic conductivities were also measured to confirm the reduction of the activation energies. The results of this study support the model for grating kinetics in rare-earth sensitized glasses proposed recently by Dixon, Hamad, and Wicksted.

DOI: 10.1103/PhysRevB.65.064204 PACS number(s): 42.70.Ce, 42.40.Eq, 42.70.Ln, 72.80.Ng

I. INTRODUCTION

Glasses sensitized with rare-earth ions are of interest for a variety of optical signal processing applications. Laser-induced permanent and transient refractive-index gratings in Eu^{3+}-doped silicate, phosphate, and germanate glasses have been previously reported.[1–13] These gratings were formed and detected using the nondegenerate four-wave mixing (FWM) technique. In all of these studies, the 465.8 nm line of a cw argon laser was used to excite the Eu^{3+} ions and a He-Ne laser to detect the grating formation. The glass compositions studied previously supported relatively weak changes in the refractive indices and required writing times of several minutes to hours to produce maximum grating efficiencies.

Previous research[1–6,11,12] supports the conclusion that the grating consists of a transient and a persistent component of different physical origin. The transient component is due to a population grating in the $^5D_0$ metastable state of Eu^{3+}.[1,11] The persistent component has been attributed to rearrangement of the glass network due to migration of small modifiers. This rearrangement is driven by the hot phonons that are emitted when Eu^{3+} decays nonradiatively from the $^5D_2$ state (reached by absorption of 465.8 nm laser light) to the $^5D_1$ and $^5D_0$ states. It should be emphasized that this hot-phonon population is nonthermal, consisting initially of the highest energy phonons in the glass (near 1300 cm^{-1} in the present case). Behrens, Durville, and Powell[4] used a tunneling model to account for the dependence of the diffracted efficiency of the permanent laser-induced grating (LIG) on the mass of the alkali modifiers in their samples. Recently, we showed that the hot phonons can force diffusion of small modifiers in the illuminated regions of the write beams and thus modify the local refractive index of the glass by modifying its composition on the scale of the fringe spacing. This model accounts well for the kinetics of grating formation and decay.[12]

The diffusion model for the formation of the persistent gratings suggests that increasing the Al concentration will improve the grating efficiencies. In crystalline quartz, a useful analog for silicate glasses, alkali impurities associated with substitutional Al are known to be mobile. Substitutional Al captures an electron from a nearby interstitial alkali to form the sp^3 hybrid orbitals needed to satisfy the tetrahedral coordination. The extra electron on the AlO_4^- complex is shared over all four tetrahedral bonds. Consequently, the center of charge on the AlO_4^- complex is further from the positively charged alkali than would be the case if it were bound to a nearest neighbor O^-; this decreases the activation energy required for alkali diffusion. This impurity complex has received extensive attention[14–19] because of its role in degrading the performance of precision quartz oscillators. In simpler silicate glasses, the substitution of Al for Si increases the ionic conductivities,[20–22] suggesting strongly that substitutional Al can play the same role in glass as it does in quartz. Thus, one is led to expect both increased ionic conductivity and, viewed from the perspective of the diffusion model, improvement in both the strength and rate of formation of holographic refractive-index gratings when the Al content of the rare-earth sensitized glasses is increased.

Here, we report a systematic study of grating formation and ionic conductivity when the Al_2O_3 concentration in an aluminosilicate glass host containing 1.26 mol% Eu_2O_3 is varied from 0 to 15 mol%. The growth, decay, and erasure of the grating are reported as functions of the Al_2O_3 concentration.

II. EXPERIMENT

All experiments were performed using the 465.8 nm laser line of a cw argon laser operating in the TEM_∞ mode as described previously by Ref. 11. The Gaussian profile of the beam was confirmed by using a laser beam profiler. A crossing angle of 10° (measured in air) was used. The write beams were focused using two lenses each of which had a 50 cm focal length. The diameter of each beam was measured to be 140 μm using the beam profiler. This corresponds to a Rayleigh range of 4.7 cm (in air).[23] The total power of the write beams was 30 mW. The read beam was focused so that its diameter at the position of the sample was about 190 μm and filled the laser-induced grating. The power of the read beam,

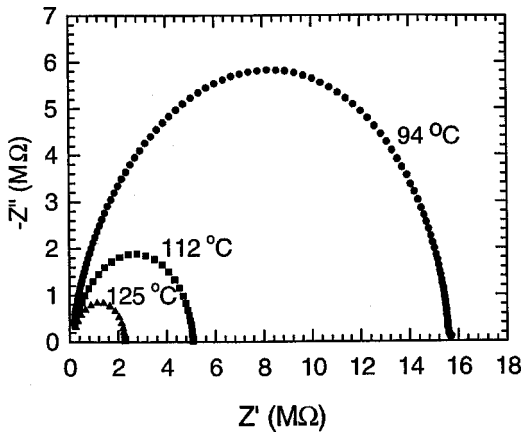

FIG. 1. Typical Nyquist plot of the complex impedances. Measurements were collected as a function of frequency from 0.1 Hz to 20 kHz: frequencies increase from right to left. The right-hand zero in Z'' occurs at the Z' corresponding to the d.c. resistance. These results are for Al-3.

P_r, at the sample surface was 3.5 mW.

Glass batch compositions were prepared from sodium carbonate, magnesium carbonate, europium carbonate, aluminum oxide, and silicon dioxide precursor powders of 99.99+% purity. All powders were mixed for approximately 1 h prior to loading into a standard form platinum crucible. The mixture was then raised to 1650 °C in a series of ramp and soak stages to allow for the decomposition of the carbonates. After soaking at 1650 °C for 50 h, the charged crucible was cooled to 1550 °C in the melting furnace at a rate of 10 °C/h. Optical quality samples were made by transferring the charged crucible into a separate annealing oven preheated to 450 °C and annealing both the crucible and its charge for 1 h at 725 °C. The annealing furnace was then turned off and allowed to cool down to room temperature. A core drill was used to remove the annealed glass from the crucible. The sample was then fine polished using cerium oxide polishing material. The batch composition of the samples was $[(73-x)SiO_2 \cdot 15Na_2O \cdot 12MgO \cdot xAl_2O_3]_{0.9874}:[Eu_2O_3]_{0.0126}$, where $x=0$, 3, 6, 9, and 15. In the following discussion, the samples are identified by the Al_2O_3 concentration (i.e., Al-0, Al-3...Al-15).

Ionic conductivities were determined by impedance spectroscopy. Samples, typically of 1 cm^2 cross section and 1 mm thickness, were polished as described above and plated with Au-Pd electrodes. They were then mounted in a temperature-controlled over. Under a 0.5 mV a.c. potential difference, the in-phase and quadrature components of the current were measured using a two-phase lock-in amplifier operating in the current mode. This allowed the real and imaginary components of the complex impedance, Z' and Z'', respectively, to be determined as a function of frequency. Fig. 1 shows typical results displayed for several different temperatures. The minimum in the Z'' vs Z' plot (Nyquist plot) occurs when Z' is equal to the d.c. resistance of the sample.

III. THEORETICAL MODEL

The experimental results will be interpreted in the light of the small modifier diffusion (SMD) model.[12] It is appropriate, then, to briefly review some of the features of this model. The reader is directed to Ref. 12 for details. In this model the persistent refractive-index contrast, $\Delta n_{\rm per}$, arises from the modulation of the local chemical composition produced by forced diffusion of small modifiers from the bright toward the dark fringes of the interference pattern. The population of hot phonons produced by nonradiative relaxation of the optically excited rare-earth sensitizers provides the energy to drive this diffusion. The rate β_I which the LIG forms is a linear function of the optical intensity (and hence, the hot-phonon density), as was experimentally verified[12] by power-dependence measurements. The maximum $\Delta n_{\rm per}$ that can be produced is proportional to the initial uniform density M_0 of mobile modifiers (bound weakly enough to be forced into diffusion by the hot phonons); to a good approximation, this maximum is independent of β_I. Both the mobile modifiers and the traps are consistent with a nonequilibrium distribution of modifiers that results from rapidly quenching the glass-forming melt from 1550 °C. The transient component, $\Delta n_{\rm tran}$, of the LIG has been shown to be an excited state population grating composed primarily of Eu^{3+} in the metastable $^5D_0$ state.[1,11]

The FWM experimental results are fit to the SMD model by solving, numerically, the coupled partial differential equations shown below:

$$\frac{\partial N(x,t)}{\partial t} = \gamma_T \phi(x,t) M(x,t)[S_T - N(x,t)] \tag{1}$$

and

$$\frac{\partial [M(x,t)+N(x,t)]}{\partial t} = \gamma_o S a^2 \frac{\partial^2}{\partial x^2}[\phi(x,t)M(x,t)]. \tag{2}$$

Here, $M(x,t)$ is the density of the mobile modifiers, $N(x,t)$ is the density of trapped modifiers, S_T is the density of deep traps, γ_T is the rate constant for the trapping, γ_o is the rate of hopping between adjacent sites, S is density of sites at which mobile modifiers are distributed, and a is the mean separation of sites. $\phi(x)$ is the density of hot phonons, which is proportional to the light intensity and given by $\phi(x) = \phi_o(2+me^{iKx}+me^{-iKx})/2$, where ϕ_o is the density of hot phonons when the light intensity is uniform. K is the wave vector of the interference pattern in the sample. The integer m is one during the writing process and zero during the optical erasure. This plane wave form for $\phi(x)$ neglects the Gaussian profile of the grating. This is not a serious limitation since, (i) all samples used in this study have the same europium content, and (ii) the grating contains many periods within the Gaussian envelope thus allowing the partial differential equations to be reduced to rate equations by transformation to Fourier space. The trapping and transport equations [Eqs. (1 and 2)] can be reduced to a set of coupled equations

$$\dot{M}_n + \dot{N}_n = -\beta_n(2M_n + mM_{n+1} + mM_{n-1}). \tag{3}$$

The change in the index of refraction as a result of the transient and persistent gratings is given by $\Delta n = \Delta n_{\rm tran} + \Delta n_{\rm per}$ where $\Delta n_{\rm per} = \sum_i n_{\rm di}(c_i/100)(\Delta M_i/\bar{M}_i)$,

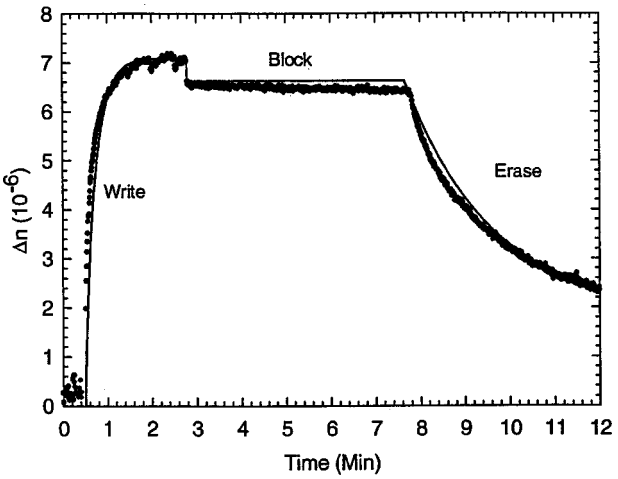

FIG. 2. Typical write-block-erase sequence. The curve is a fit to the data using Eq. (3) of the model with the model parameters $\beta_1 = 0.257\ s^1$ and $M_0 = 2.83 \times 10^4\ cm^{-3}$. These results are for Al-6.

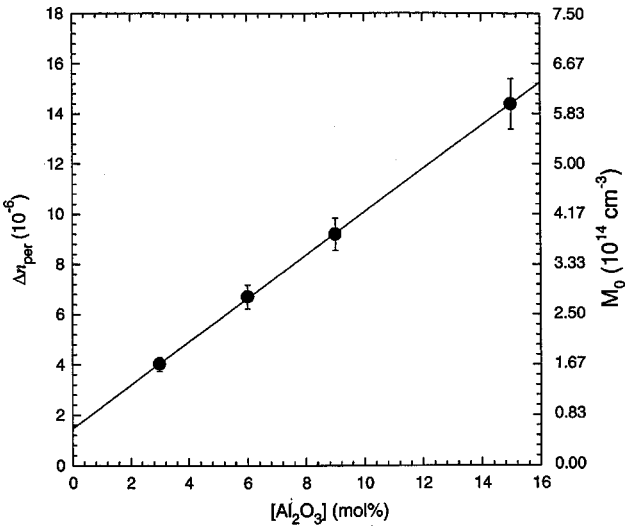

FIG. 3. Dependence of the persistent grating strength on the Al_2O_3 concentration. The linear dependence on $[Al_2O_3]$ is predicted by the small-modifier-diffusion model. M_0 is the concentration of mobile modifiers required to produce the observed persistent grating strength using the model.

where c_i is the concentration of the component oxide in mol.% and n_{di} is its contribution to the index of refraction, $\overline{M}_i$ is the mean total density of the ith chemical species.

The fitting parameters used are $\beta_i = \gamma_o \phi_o S K^2 a^2/2$, the rate of growth and optical erasure of the persistent grating, and M_o the mean density of mobile modifiers. The trapping parameter, γ_T, is important only for extended write times and was unnecessary in the present study.

IV. RESULTS AND DISCUSSION

The samples used in this study have different thicknesses and absorption coefficients. Also, in our experiment, the overlap of the write beams is larger than the sample thickness; therefore, the grating length is equal to the sample thickness and differs in each of these samples. Since the diffracted signal intensity is dependent on the grating length and absorption, it would not be accurate to compare the results of the samples according to their diffraction efficiencies. Therefore, we compared them using the induced change in the index of refraction, calculated using the method of Hamad and Wicksted,[24] which accounts for sample thickness, absorptivity, and the Gaussian profiles of the beams. This enabled us to determine the role of the Al_2O_3 concentration on the refractive-index contrast, which is responsible for the diffraction efficiencies.

Typical results for a write-block-erase cycle are shown in Fig. 2 for the Al-6 sample. When the write beams were turned on, the diffracted signal appeared immediately and reached its maximum rapidly. At this point, if the write beams were kept on, the signal intensity decayed slowly. As we have shown elsewhere,[12] this behavior is consistent with random-walk diffusion in a medium containing a low density of deep traps. In general, the decay rate of the signal was dependent on the Al_2O_3 concentration. When the write beams were blocked after the diffracted intensity reached its maximum, the signal decayed quickly to a persistent level. Erasure of the persistent grating was accomplished by unblocking one of the write beams. The curve through the data shown in Fig. 2 is a fit of the small-diffusion-modifier model developed by Dixon, Hamad, and Wicksted.[12] The rate constant, β_1, for the growth and optical erasure of the persistent grating and the density of mobile modifiers, M_0, in Eq. (3) were treated as adjustable parameters to obtain the fit. Data similar to that shown in Fig. 2 were collected for each of the Al concentrations.

Fig. 3 displays the Al concentration dependence of the change in the index of refraction due to the persistent grating formation. Δn_{per} is the value of Δn immediately after the write beams were blocked. The data clearly show that the grating strength increases linearly with increasing Al_2O_3 concentration in the melt. According to the small-modifier diffusion model,[12] the change in the index of refraction observed by first-order Bragg scattering of the probe beam is proportional to the first-order Fourier component of the local density of modifiers that are able to diffuse under the influence of the laser interference pattern. This, in turn, is proportional to the total mobile modifier density which, as we noted above, is expected to increase linearly with the density of substitutional Al. The observed linear increase in Δn_{per} confirms this prediction of the diffusion model. The right-hand axis of Fig. 3 displays the corresponding mobile modifier densities for the various sample compositions. One notes that the *mobile* modifiers represent only a fraction of the Na bound to AlO_4^- clusters. This is to be expected since in addition to a reduced binding energy to the cluster there must also be nearby Eu^{3+} on resonance with the laser to provide excitation and an open channel for the Na to migrate along the intensity gradient.

This picture of the role of Al in increasing the number of weakly bound modifiers is further validated by the ionic conductivities of these glasses. Fig. 4 shows an Arrhenius plot of

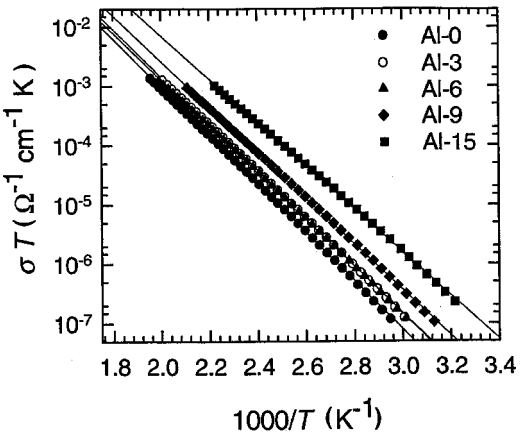

FIG. 4. Ionic conductivities determined by impedance spectroscopy for the several sample compositions. These also demonstrate an increase in mobile small modifiers as $[Al_2O_3]$ increases.

the ionic conductivities of the compositions studied optically. Clearly, the addition of Al_2O_3 causes an increase in the ionic conductivities of these glasses. The average activation energies for ionic diffusion are obtained from the slopes of the Arrhenius curves. These activation energies are displayed in Fig. 5 and demonstrate that the small modifiers responsible for the ionic conductivity are, on average, less strongly bound as the Al concentration increases.

Even with no Al doping, it is still possible to write a weak grating, indicating that alkalis associated with Al are not the only mobile modifiers. Likewise, there is a nonvanishing ionic conductivity in the absence of Al. In discussing the ionic conductivity of aluminosilicate glasses, Greaves and Ngai[22] have proposed two mechanisms for the alkali ions to migrate through the network. In the first of these, termed intrachannel hopping, the alkalis are coordinated to nonbridging oxygens (NBO's). Alkali migration is accompanied by a redistribution of bonds so that NBO's follow the migrating alkalis to minimize the electrostatic energy of the network. In other words, some of the NBO's exchange with bridging oxygens (BO's). The second, network hopping, occurs when the alkalis are associated with the AlO_4^- groups,

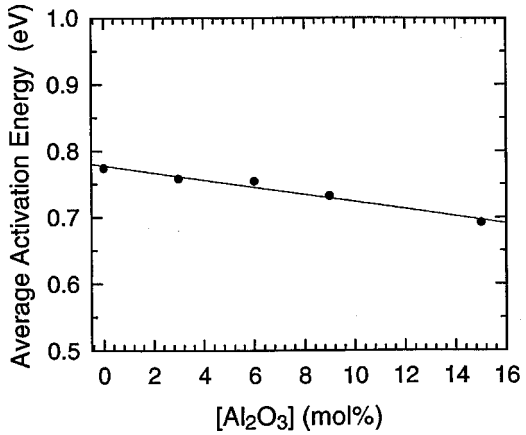

FIG. 5. Activation energies for ionic motion determined from the data of Fig. 4. The line is a guide to the eye.

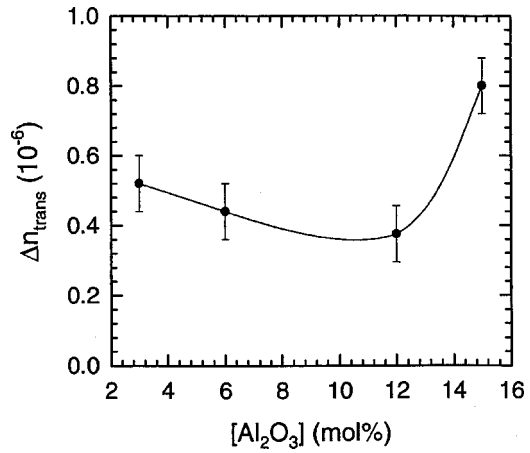

FIG. 6. Transient grating strength as a function of $[Al_2O_3]$. The Δn_{trans} for the three lowest concentrations are not distinguishable within experimental uncertainty. The curve is a guide to the eye.

i.e., the alkalis are coordinated to BO's. In this case, small configurational changes occur due to the alkali migration. In the absence of Al, only the first of these mechanisms can occur. In the aluminosilicate glasses, both mechanisms are possible.

The dependence of the transient component of the gratings on Al_2O_3 concentration in the melts is shown in Fig. 6. This is seen to increase slightly at the largest Al concentration. We interpret this as resulting from either an increased population in Eu ions with their $^5D_2$ states on resonance with the laser and/or to an increased branching ratio for nonradiative decay to the $^5D_0$ state. Both of these could result from an increase in favorable Eu environments in the network. In either case, there will be an increase in the number of hot phonons generated to stimulate diffusion of small modifiers.

Figure 7 displays the Al dependence of the buildup times of the grating for formation of the maximum grating (τ_{max}) and for formation of 50% of the maximum grating (τ_{50}). The much longer times to maximum Δn are expected because of the gradual depletion of mobile modifiers in the illuminated

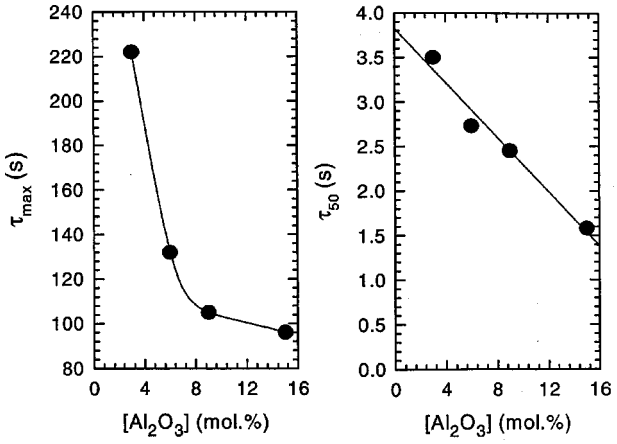

FIG. 7. Rise times for grating formation to maximum and 50% maximum grating strength. Both decrease with increasing $[Al_2O_3]$. The curves are guides to the eye.

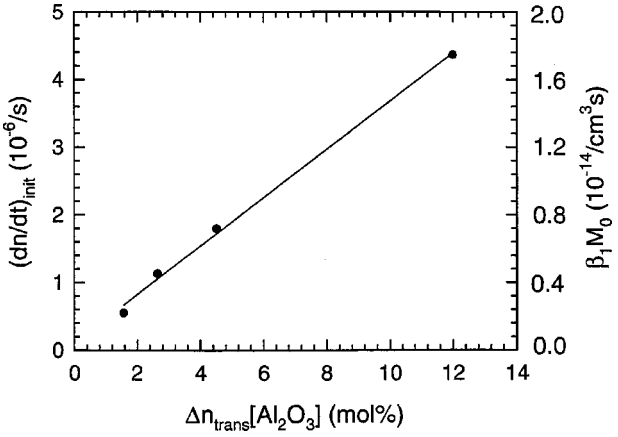

FIG. 8. Comparison of the initial growth rate of the gratings with the prediction of the small-modifier-diffusion model as discussed in the text. The line is a least squares fit to the data. The right-hand axis represents the growth rate, $\beta_1 M_0$, of the first-order Fourier component of the nonuniform modifier distribution used in the model.

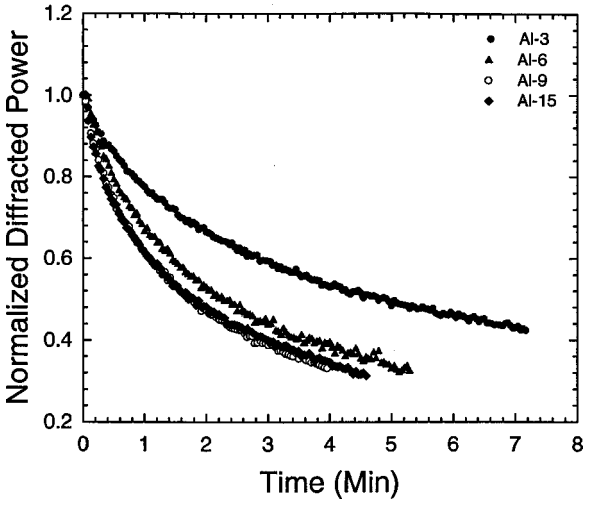

FIG. 9. Normalized erasure curves for the several compositions. The erasure rate increases rapidly with increasing $[Al_2O_3]$ at low concentrations, but appears to have saturated by 9% $[Al_2O_3]$.

regions as the grating develops. In the diffusion model[12] for grating kinetics, the initial rate for grating formation is proportional to both the initial density of mobile modifiers and to the density of hot phonons. Thus, it is expected that the initial rates for our glasses will be a linear function of the product of Δn_{trans} and the Al_2O_3 concentration in the melt. Using $\Delta n_{per}(50\%)/\tau_{50}$ as an estimate of the initial rate, this linear relationship is displayed in Fig. 8.

Figure 9 displays the erasure of the persistent induced change in the index of refraction for the set of samples used in this study. The erasure rate, like the rate of grating formation, is faster for the samples with higher Al_2O_3 concentration. During the erasing process, the dark regions (regions that were dark fringes during the writing process) as well as the bright regions (regions that were bright fringes during the writing process) are illuminated. Therefore, the processes of structural and compositional change that took place in the bright regions now occur in the dark regions as well. In addition, the bright regions experience structural changes due to the redistribution of the mobile modifiers. As the figure shows, the rate of structural and compositional change slows as ever-more-tightly-bound modifiers must be moved. These changes remove the spatial modulation of the refractive index caused by the writing process, but, as we have noted above, do not reestablish the original nonequilibrium distribution of modifier energies. Thus, there will remain a persistent lens due to the Gaussian profile of the erasure beam[25]

V. SUMMARY AND CONCLUSIONS

In this paper, we have shown that the evolution of the strength and kinetics of holographic refractive-index gratings in Eu-sensitized aluminosilicate glasses with increasing Al concentration is well described by the diffusion model.[12] The role of Al in increasing the concentration of mobile modifiers, as inferred from studies of analogous centers in crystalline quartz, is confirmed by the increasing ionic conductivities and decreasing activation energies that accompany higher Al concentrations. These results indicate that the diffusion model contains the essential physics of the grating formation process.

ACKNOWLEDGMENTS

This material is based upon work supported in part by the US Army Research Office under Grant No. DAAH04-96-1-0322 and the NSF under Grant No. DMR9705284

*Permanent address: Department of Physics, Box 1654, Southern Illinois University, Edwardsville, IL 62026-1654.

†Michael Hogsed, Air Force Research Laboratory/VSSE, 3550 Aberdeen Ave. SE, Bldg. 914, Kirtland AFB, NM 87117-5776.

[1] F. M. Durville, E. G. Behrens, and R. C. Powell, Phys. Rev. B **34**, 4213 (1986).

[2] F. M. Durville, E. G. Behrens, and R. C. Powell, Phys. Rev. B **35**, 4109 (1987).

[3] E. G. Behrens, F. M. Durville, and R. C. Powell, Opt. Lett. **11**, 653 (1986).

[4] E. G. Behrens, F. M. Durville, and R. C. Powell, Phys. Rev. B **39**, 6076 (1989).

[5] E. G. Behrens, R. C. Powell, and D. H. Blackburn, Appl. Opt. **29**, 1619 (1990).

[6] E. G. Behrens, R. C. Powell, and D. H. Blackburn, J. Opt. Soc. Am. B **7**, 1437 (1990).

[7] V. A. French, R. C. Powell, D. H. Blackburn, and D. C. Cranmer, J. Appl. Phys. **69**, 913 (1991).

[8] A. Munoz F., R. J. Reeves, B. Taheri, R. C. Powell, Douglas H. Blackburn, and David C. Cramer, J. Chem. Phys. **98**, 6083 (1993).

[9] M. M. Broer, A. J. Bruce, and W. H. Grodkiewicz, J. Lumin. **53**,

15 (1992).
[10] M. M. Broer, A. J. Bruce, and W. H. Grodkiewicz, Phys. Rev. B **45**, 7077 (1992).
[11] A. Y. Hamad, J. P. Wicksted, and G. S. Dixon, J. Non-Cryst. Solids **241**, 59 (1998).
[12] G. S. Dixon, A. Y. Hamad, and J. P. Wicksted, Phys. Rev. B **58**, 200 (1998).
[13] A. Y. Hamad, J. P. Wicksted, and G. S. Dixon, Opt. Mater. **12**, 41 (1999).
[14] A. Kahan, F. E. Euler, H. G. Lipson, C. Y. Chen, and L. E. Halliburton, in *Proceedings of the 41st Annual Symposium on Frequency Control* (IEEE, Piscataway, N.J., 1987), p. 216.
[15] H. D. Nutall and J. A. Weil, Can. J. Phys. **59**, 1696 (1981); **59**, 1709 (1981); **59**, 1886 (1981).
[16] M. J. Mombourquette, J. A. Weil, and P. G. Mezey, Can. J. Phys. **62**, 21 (1984).
[17] M. J. Mombourquette and J. A. Weil, Can. J. Phys. **63**, 1282 (1984).
[18] T. M. Wilson, L. E. Halliburton, M. G. Jani, and J. J. Martin, in *Proceedings of the 40th Annual Symposium on Frequency Control* (IEEE, Piscataway, N.J., 1986), p. 26.
[19] T. M. Wilson, J. A. Weil, and P. S. Rao, Phys. Rev. B **34**, 6053 (1986).
[20] C. H. Hsieh and H. Jain, J. Non-Cryst. Solids **183**, 1 (1995).
[21] L. Cormier, P. H. Gaskell, G. Calas, J. Zhao, and A. K. Soper, Phys. Rev. B **57**, 8067 (1998).
[22] G. N. Greaves and K. L. Ngai, Phys. Rev. B **52**, 6358 (1995).
[23] E. A. Saleh and M. C. Teich, *Fundamentals of Photonics* (Wiley, New York, 1991).
[24] A. Y. Hamad and J. P. Wicksted, Opt. Commun. **138**, 354 (1997).
[25] F. M. Durville and R. C. Powell, J. Opt. Soc. Am. B **4**, 1934 (1987).